



A safe and efficient bioactive citrate-lysine/miRNA33 agonist nanosystem for high fat diet-induced obesity therapy

Long Zhang^a, Min Wang^a, Mi Chen^a, Wen Niu^a, Wenguang Liu^a, Tongtong Leng^a,
Wenchen Ji^e, Bo Lei^{a,b,c,d,*}

^a Department of Pulmonary and Critical Care Medicine, The Second Affiliated Hospital of Xi'an Jiaotong University, Frontier Institute of Science and Technology, Xi'an Jiaotong University, Xi'an 710054, China

^b Key Laboratory of Shaanxi Province for Craniofacial Precision Medicine Research, College of Stomatology, Xi'an Jiaotong University, Xi'an 710000, China

^c National and Local Joint Engineering Research Center of Biodiagnosis and Biotherapy, The Second Affiliated Hospital of Xi'an Jiaotong University, Xi'an 710000, China

^d Instrument Analysis Center, Xi'an Jiaotong University, Xi'an 710054, China

^e Department of Orthopedics, The First Affiliated Hospital of Xi'an Jiaotong University, 710061, China

ARTICLE INFO

Keywords:

Bioactive biomaterials
Polycitrate
miRNA delivery
Obesity therapy

ABSTRACT

The increased prevalence of obesity is recognized as a serious public health problem affecting millions of people. Although some anti-obesity drugs are currently licensed for use, these drugs involve diverse side effects such as diarrhea, vomiting, and low efficiency. Here we developed a safe and efficient biomaterials-based anti-obesity nanosystem (PCG-EPL/miR33agonist), which was formed with poly (citric acid)-glycerol-polylysine (PCG-EPL) and miR33 agonist by self-assembly. The PCG-EPL could efficiently load, protect and deliver the miR33 agonist into the adipocytes and decreased the obesity-related IL-1 β expression in adipocytes *in vitro*. The high-fat diet induced obese rat model experiment showed that the PCG-EPL/miR33agonist *via* caudal vein injection effectively reduced the body weight by enhancing lipid metabolism and decreasing the inflammatory factors expressions (IL-1 β , TNF- α and IL-6) *in vivo*, without suppressing the appetite of rat. Compared with the obese mice, mice in PCG-EPL/miR33 had higher average food intake but lower energy conversion rate. PCG-EPL/miR33agonist significantly inhibited the growth of adipocytes. Noteworthy, this weight loss strategy is not only safe and efficient, but also does not need diet control. Thus, PCG-EPL may serve as an ideal platform for RNA drug delivery in anti-obesity therapy, especially for those who need to lose weight but unable to autonomously control their diet.

1. Introduction

The increased prevalence of obesity is now considered to be as one of the most serious public health problems affecting millions of people [1,2]. The obesity usually results from a positive imbalance of energy metabolism, which occurs when the amount of energy ingested exceeds the amount expended [3]. Obesity is also closely linked to the incidence of metabolic syndromes such as cardiovascular disease, type-2 diabetes, hypertension, nonalcoholic fatty liver disease, dyslipidemia, atherosclerosis and acute myocardial infarction [4]. Compared with surgical weight loss, the anti-obesity pharmacotherapy is a potentially important adjunctive treatment to improve the life quality of patients due to its ease of use, low cost, and high patient compliance. Although some anti-obesity drugs such as sibutramine and rimonabant are currently licensed for long-term use, these drugs involve diverse side effects such as

diarrhea, vomiting, and low efficiency [1]. Therefore, the development of safe and efficient anti-obesity drug can not only improve the quality of life of obese patients, but also help prevent the disease progression into other chronic diseases.

Gene drugs such as miRNAs play important roles the in metabolic organs such as liver and adipose tissue. Gene medicine has advantages in medical application due to its strong targeting and small side effects [5]. Regulatory miRNAs have also emerged as important modulators for fat metabolism [6]. Previous studies have shown that miR33 is closely related to obesity [6–8]. Genetic ablation of miR33 increases the food intake/adipose tissue expansion, and promotes insulin resistance/obesity [8]. By regulating the expression of leptin, insulin and lipoprotein, miR33 can control the lipid metabolism [6–10]. Therefore, we hypothesize that regulating miR33 expression may be a potential breakthrough for obesity therapy. Gene therapy has become an

* Corresponding author at: Frontier Institute of Science and Technology, Xi'an Jiaotong University, Xi'an 710054, China.

E-mail address: rayboo@xjtu.edu.cn (B. Lei).

attractive method to restore tissue functions and diseases treatment [11]. How to effectively and safely transfer therapeutic genes such as miRNA or siRNA into target cells or tissues was a major obstacle for successful application of gene therapy. Due to the versatility, biomaterials-based nanotechnology has exhibited promising application in gene therapy for disease treatment [12–14]. Compared with conventional viral vehicle, biomaterials mediated drug delivery systems have been widely used in the treatment of obesity or cancer [15–17]. Among them, polymer biomaterials-based vehicles could effectively load drugs/or genes and increase their efficiency. Therefore, the polymer biomaterials-based nanosystem could be potentially used for obesity therapy by the targeted miRNA delivery.

Conventional polymer biomaterials gene vehicles such as dendrimer, micelles and poly (beta-amino ester) exhibited various disadvantages including cytotoxicity and non-biodegradable (dendrimers and micelles) and limited tissue penetration and controlled release of cargo release (poly-beta-amino ester) [18–20]. Polycitrate (PC)-based polymers (PCBP) have been investigated extensively in biomedicine because of the low cost and high biocompatibility/biodegradation [21]. However, PCBP-based biomaterials are hydrophobic and have no capacity to load and release miRNA for potential application in gene therapy [22]. In our previous study, we synthesized an amphiphilic polycitrate-polyglycol-polyamine (PCGE) copolymer as the vehicle for gene delivery and obtained excellent efficiency in tissue regeneration [23]. However, the polyamine in the structure was still not biodegradable and had potential cytotoxicity [24,25].

As an anti-microbial polypeptide, epsilon-poly-l-lysine (EPL) is biodegradable, antibacterial and biocompatible, which has the potential gene delivery ability [26]. Therefore, it is reasonable and promising to develop the safe and efficient PCG/EPL-based vehicle to deliver miRNA for anti-obesity therapy. Herein, we develop the polycitrate-polyglycerol-EPL (PCG-EPL) co-polymers, and investigate their capacity to deliver miR33 agonist to regulate the function of adipocyte and treat the high-fat diet induced obesity.

2. Materials and methods

2.1. Synthesis of PCG-EPL

Citric Acid (99%), 1,8-Octanediol (98%) and polyethylene glycol (PEG) (1 kDa) were used for PCG synthesis according to the previous report [23]. The PCG-EPL was synthesized using PCG and poly- ϵ -lysine (EPL) under catalytic reaction of 1-(3-Dimethylaminopropyl)-3-ethylcarbodiimide (EDC, 99%) and N-Hydroxysuccinimide (NHS, 98%) in a buffer solution (pH 5–6). Briefly, the carboxyl groups of PCG were activated by EDC for 30 min, and reacted with EPL at the room temperature for 24 h. The PCG prepolymer and PCG-EPL was dialyzed by the dialysis tube for 2 d (MWCO 3500), followed by freeze-drying. The physicochemical structure of PCG-EPL polymer was analyzed by ^1H nuclear magnetic resonance (^1H NMR) (Ascend 400 MHz, Bruker) and the Fourier transformation infrared (FT-IR) instrument (NICOLET 6700, Thermo). All chemical reagents were purchased from Sigma-Aldrich.

2.2. Preparation and characterization of PCG-EPL/miRNA complexes

In order to find the best combination ratio of PCG-EPL and miRNA, miRNA33 agomir (RiboBio, China) and PCG-EPL with different ratios was mixed and incubated at 37 °C for 30 min to obtain self-assembled PCG-EPL/miRNA. The miRNA binding ability, release and stability from PCG-EPL were measured using the agarose gel retardation assay. For miRNA binding ability detection, we blended 1 μL miRNA (20 μM) with different doses of PCG-EPL (10 $\mu\text{g}/\mu\text{L}$) (0, 0.25, 0.5, 1, 2, 4, 6, 8, 10, 20 μL). The binding ratio of miRNA to PCG-EPL was detected using agarose gel assay.

The stability of PCG-EPL/miRNA was analyzed by the heparin sodium [21]. The complexes solution with v/v ratio of 4:1 (PCG-EPL/

miRNA was assembled with 4 μL PCG-EPL and 1 μL 20 μM miRNA) was cultured with the heparin sodium salt at various concentrations (0, 0.31, 0.63, 1.25, 2.5, 5, 10 $\mu\text{g}/\mu\text{L}$) for 1 h at 37 °C. Fetal bovine serum (FBS, cat No.10091148, Gibco, New Zealand) solution was used to test the degradation stability of PCG-EPL/miRNA. The complexes solution (v/v = 4, 4 μL PCG-EPL and 1 μL 20 μM miRNA) was incubated with 5 μL FBS solution at 37 °C for indicated time intervals (0, 1, 4, 8, 12, 24 h and naked miRNA at 1 h). Then the mixtures were cultured with heparin sodium salt (10 $\mu\text{g}/\mu\text{L}$) for another 1 h at 37 °C. The particle size/zeta potential of PCG-EPL/miRNA was tested through the dynamic light scattering (Zetasizer, Malvern Instruments). The particle morphology of PCG-EPL/miRNA complexes was determined by the transmission electron microscopy (TEM) (H-8000, Hitachi).

2.3. Cytotoxicity and gene transfection ability

3T3-L1 pre-adipocytes (ATCC, USA) were employed for the cytotoxicity analysis. Cells were cultured in a 96-well plate (7000 cells/well) in a high glucose Dulbecco's culture medium (DMEM, HyClone) with 10% FBS (Gibco) (37 °C, 5% CO_2). After 24 h, culture medium was replaced by DMEM containing 10% FBS and different concentrations of PCG-EPL (0, 5, 10, 20, 50, 100, 125 and 150 $\mu\text{g}/\text{mL}$). Subsequently, the cell viability was investigated using CCK-8 assay (cat No. C0038, Beyotime, China) by determining the fluorescent intensity with a microplate reader (Thermo Fisher) at 450/630 nm (excitation/emission) after 24 h incubation. The cytotoxicity of PCG-EPL (50 $\mu\text{g}/\text{mL}$) on 3T3-L1 was detected at different time points (0, 4, 8, 12, 24, 48 h). And cell uptake ability of PCG-EPL/miRNA was evaluated both in 293T and 3T3-L1 cells. The formulated PCG-EPL/cy3miRNA (miRNA:20 nM, PCG-EPL:40 $\mu\text{g}/\text{mL}$) was added into the 293T or 3T3-L1 pre-adipocytes culture medium (10% FBS in DMEM and 1% penicillin streptomycin), and incubated for 24 h (37 °C, 5% CO_2). Photos were collected to verify the cell uptake ability of PCG-EPL/miRNA by using commercial transfection agent Lipofectamine2000 (Lipo2000, Thermo) as a control.

2.4. Adipocyte cell culture and differentiation

3T3-L1 pre-adipocytes were cultured at 37 °C under 5% CO_2 in DMEM medium containing 10% FBS and 1% penicillin streptomycin (cat No.15140122, Gibco). Differentiation was induced for 2 days by adding DMEM containing 10% FBS and 1% penicillin streptomycin supplemented with 0.5 mM 3-isobutyl-1-methylxanthine (IBMX, Sigma), 1 μM dexamethasone (Sigma) and 10 $\mu\text{g}/\text{mL}$ insulin (Sigma) for 2 days, and then continued to be cultured in the medium containing 10% FBS, 1% penicillin streptomycin and 10 $\mu\text{g}/\text{mL}$ insulin for another two days. Then culture medium (DMEM containing 10% FBS and 1% penicillin streptomycin) was changed every two days for 2 times.

2.5. Functional detection of PCG-EPL/miR33 in vitro

The function of PCG-EPL/miR33 was evaluated by RT-qPCR and Oil-Red O Staining in adipocytes using commercial transfection agent Lipo2000 as a control. 20 nM of miR33mimic or miR33mimic NC (miR33mimic negative control) was respectively transfected into adipocytes (induced from 3T3-L1 pre-adipocytes) according to the following transfection combination strategy: miR33mimic, PCG-EPL/miR33 mimic NC, Lipo2000/miR33 mimic and PCG-EPL/miR33 mimic (40 $\mu\text{g}/\text{mL}$ of PCG-EPL). After 24 h treatment, the gene expression was detected by real-time PCR method. Primers information was shown in Table S1. And Oil-Red O Staining was used to detect the lipid expression. Quantification of oil drop area by ImageJ software (HIH, for Windows).

2.6. Mice and diets

The male C57BL/6 mice (8 weeks) were obtained from the Animal

Centre in Xi'an Jiaotong University. All mice experiments were agreed by the (ACUC) Animal Care and Use Committee in XJTU. After one week's acclimation on a normal chow diet, mice were divided into two groups. One group was fed with normal chow diet and the other group was fed with high fat diet (HFD, D12492, 60% fat, Research Diets) to generate obese model mice. Compared with normal chow diet group (NCD, $n = 7$), mice with more than 30% weight gain were randomly divided into HFD-Ctrl and HFD-Exp group (high-fat diet, $n = 7$). During the preparation of obese model mice, the mice with weight gain lower than 10% of NCD group were regarded as the obese-free mice (HFD-L). These mice were not obese even though they were fed with high-fat diet. In order to study the obese-free mice, we listed them in a single group (HFD-L, which was fed high-fat diet in the whole process, $n = 7$). Mice were injected with PBS or 10 mg/kg PCG-EPL/miRNA ($v/v = 4$) through the tail vein every two days according to the following strategy: 1) NCD (normal chow diet control) treated with PBS; 2) HFD-L (high fat diet but obese-free) treated with PCG-EPL/miR33 negative control agomir (RiboBio, Guangzhou, China); 3) HFD-Ctrl (high fat diet, control group) treated with PCG-EPL/miR33 negative control agomir; 4) HFD-Exp (high fat diet, experimental group) treated with PCG-EPL/miR33 agomir. Both miR33 mimic and miR33 agomir are miRNA33 agonists. The difference was that miR33 mimic was often used *in vitro*, while miR33 agomir is used for *in vivo* study. The blood glucose, body weight and food intake were recorded from day 0 to day 21. GTT was tested on day 20 ($n = 3$). And serum samples, abdominal fat, liver, spleen and lung were collected on day 21.

2.7. Glucose tolerance test

After 20 days of administration of anti-obesity materials, three mice in each group were randomly selected to fast overnight. The blood glucose level was measured at 0, 15, 30, 60 and 120 min after injected with 2 g/kg glucose intraperitoneally on day 21 (ACCU-CHECK, Roche Diagnostics).

2.8. ELISA and RT-PCR assay

On day 21, the enzyme linked immunosorbent assay (ELISA) analysis was carried out on the serum sample. High density lipoprotein (HDL, Hengyuan), low density lipoprotein (LDL, Hengyuan), leptin (RD) and insulin (Alpco) were measured according to the manufacturers' instruction. Three repeats were used and the microplate reader was used to test the signal (Thermo Fisher). Total RNA was isolated and purified using RNAiso Plus (TaKaRa) from abdominal fat (WAT, white adipose tissue) and liver. And cDNA was synthesized using the Transcriptor First Strand cDNA Synthesis Kit (Roche) in accordance with the manufacturer's instructions. Primers information was shown in Table S1.

2.9. Histological analyses

The histological analysis was employed on the samples of abdominal fat, liver, spleen and lung tissues. Samples were fixed overnight with 4% paraformaldehyde and dehydrated, paraffin-embedded, cut into 4 μm serial sections and mounted on slides before H&E and immunofluorescence staining. For immunofluorescence staining, the sections were deparaffinised with xylene and rehydrated by immersion into decreasing concentrations of ethanol. Tissue sections were placed in EDTA antigen repair buffer (pH 8.0) for antigen repair in microwave oven. Nonspecific protein binding was blocked by with 5% bovine serum albumin (Vetec) for 30 min. Then the samples were respectively incubated with primary antibody (IL-1 β , PPAR- γ , Leptin, Servicebio and Adiponectin from Proteintech) and the matched fluorescence labeled second antibody (Cy3 labeled Goat anti rabbit and FITC labeled Goat anti mouse). And the samples were washed with PBS for three times after each step of antibody incubation.

2.10. Statistical analysis

All statistical experimental results were expressed as means \pm SD and treated through a software (Prism version 7, GraphPad Software Inc.). An unpaired two-tailed Student's *t* test and two-way ANOVA (Sidak's multiple comparisons test) were used for comparisons between groups. A *P* value of < 0.05 was considered statistically significant.

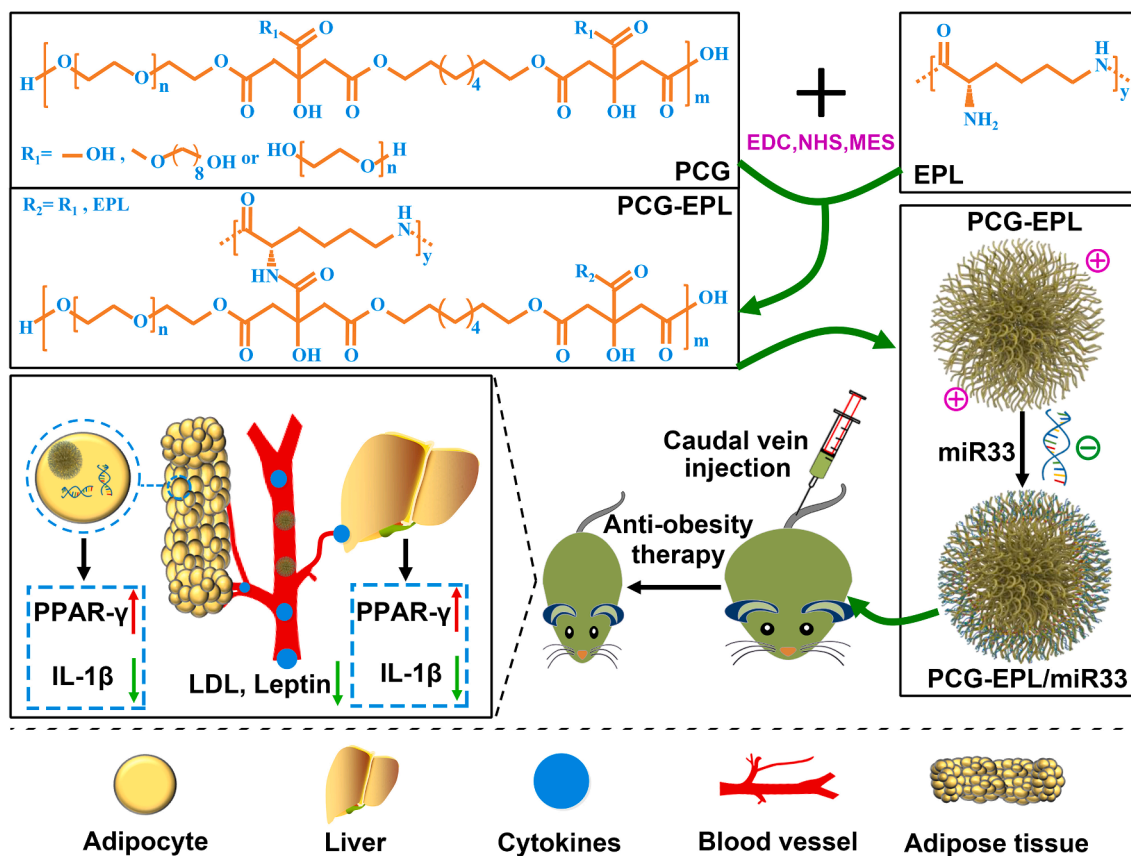
3. Results

3.1. Synthesis and characterization of PCG-EPL copolymer

Scheme 1 describes the synthesis of PCG-EPL and PCG-EPL/miR33, and the principle of PCG-EPL/miR33 in obesity therapy. PCG-EPL was synthesized with poly- ϵ -lysine (EPL) and PCG that synthesized with citric acid, 1,8-octanediol and polyethylene glycol (PEG) (Fig. S1 and Scheme 1). PCG-EPL polymer was synthesized by two steps of chemical reaction. Firstly, PCG was synthesized by thermal polymerization of citric acid, 1,8-octanediol and polyethylene glycol (Fig. S1), and then PCG-EPL was synthesized by catalytic reaction of PCG and EPL. The chemical structure of PCG-EPL was determined by ^1H NMR analysis (Fig. 1A). The multiple peaks between 2.3 and 2.9 ppm were identified as the methylene ($-\text{CH}_2-$) of CA. The peak at 3.6 ppm was attributed to the methylene ($-\text{CH}_2-$) of PEG. The multiple peaks between 1.1 and 1.6 were assigned to the methylene ($-\text{CH}_2-$) of OD and EPL. The peak at 3.1 ppm was identified as the methylene ($-\text{CONH}-\text{CH}_2-$) connected to amido bond of EPL. The peak at 3.3 ppm was belonged to the methine ($-\text{CH}-$) of EPL. The multiple peaks between 3.9 and 4.3 ppm were identified as the methylene ($-\text{COO}-\text{CH}_2-$) connected to the ester bond of, indicating the successful synthesis of PCG prepolymer. In addition, the molar ratio of CA, OD, PEG and EPL calculated from ^1H NMR was 1.00:0.67:0.32:0.18. The chemical structure of PCG-EPL polymer was further characterized by FTIR analysis (Fig. 1B). The peaks at 3240 cm^{-1} and 1560 cm^{-1} were belonged to the amino ($-\text{NH}-$) of EPL. The peak at 1740 cm^{-1} was assigned as the ester bonds ($-\text{COO}-$) of PCG and PCG-EPL polymer, further indicating the successful synthesis of PCG prepolymer. The absorption peak of amido bond ($-\text{CONH}-$) moved from 1670 cm^{-1} to 1648 cm^{-1} between EPL and PCG-EPL, indicating the successful synthesis of PCG due to the absorption of amide bond shifted by further acylation reaction.

3.2. Fabrication and evaluation of PCG-EPL/miR33mimic nanocomplex

The formation and characterizations of PCG-EPL/miR33mimic nanocomplex are showed in Fig. 2. The miR33mimic binding and complexes stability evaluation of PCG-EPL at different v/v ratios were carried out by agarose gel electrophoresis. PCG-EPL could completely bind miRNA at the v/v ratio of 4 (Fig. 2A-B), suggesting the good gene binding performance. To detect the release of miR33mimic from PCG-EPL/miR33mimic nanocomplex, the heparin sodium salt was employed as a polyanion. The miR33mimic could be highly released from PCG-EPL when the heparin sodium salt concentration was higher than $2.5\text{ }\mu\text{g}/\mu\text{L}$ (Fig. 2C-D). The FBS solution was used to assay the stability of PCG-EPL/miRNA. After different times interval treatment in FBS, we found that miR33mimic still be protected by PCG-EPL after 24 h incubation (Fig. 2E-F), but the naked miR33mimic was almost degraded completely after soaking for 1 h. After mixing PCG-EPL and miR33mimic, the self-assembly spherical nanocomplex with mean size of 220 nm was formed at the v/v ratio of 4 (Fig. 2G). The average size and zeta potential of PCG-EPL/miR33mimic are shown in Fig. S2. The pre-adipocytes (3 T3-L1) were employed to analyze the cytotoxicity of PCG-EPL. We used different concentrations of PCG-EPL to treat 3 T3-L1 cells to detect the cytotoxicity. And our results showed that PCG-EPL showed no cytotoxicity at the dose below $50\text{ }\mu\text{g}/\text{mL}$ (Fig. 2H). When the concentration of PCG-EPL was decreased into the $100\text{--}150\text{ }\mu\text{g}/\text{mL}$, the cell viability was about 70%–75% which was significantly low



Scheme 1. Schematic depiction for the synthesis of PCG-EPL/miRNA and the application of PCG-EPL/miR33 agonist in obesity therapy.

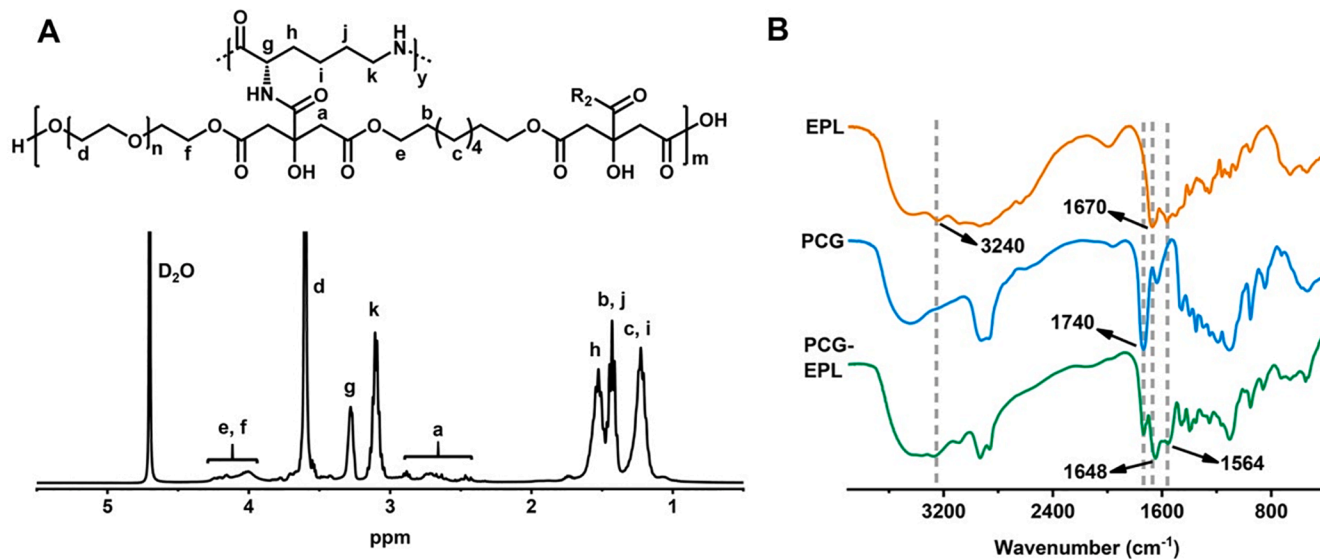


Fig. 1. Physicochemical structure evaluation of PCG-EPL polymer. (A) 1H NMR spectra of PCG-EPL polymer. (B) FTIR spectra of EPL, PCG and PCG-EPL polymer.

compared with PCG-EPL groups at low concentrations. Additionally, the 3 T3-L1 cells viability did not show significant decrease after treatment for different time points (0–48 h) by the PCG-EPL (50 μ g/mL) (Fig. 2I). These results indicated that PCG-EPL was cytotoxic at a certain concentration. The cell uptake ability of PCG-EPL/miRNA was tested both in 293T and 3T3-L1 cells (Fig. 3). Compared with commercial transfection reagent Lipo2000 and naked miRNA, PCG-EPL showed the higher intracellular delivery (red fluorescence) efficiency both in 293T

(Fig. 3A-B) and 3T3-L1 cells (Fig. 3C-D).

3.3. Regulation of gene expression in adipocytes in vitro

Fig. 4 shows the effect of PCG-EPL/miR33 on the lipid and related genes expression in adipocytes that induced from 3T3-L1 pre-adipocytes. The commercial gene transfection agent (Lipo2000) was used as a control. Compared with the control groups (miR33mimic and

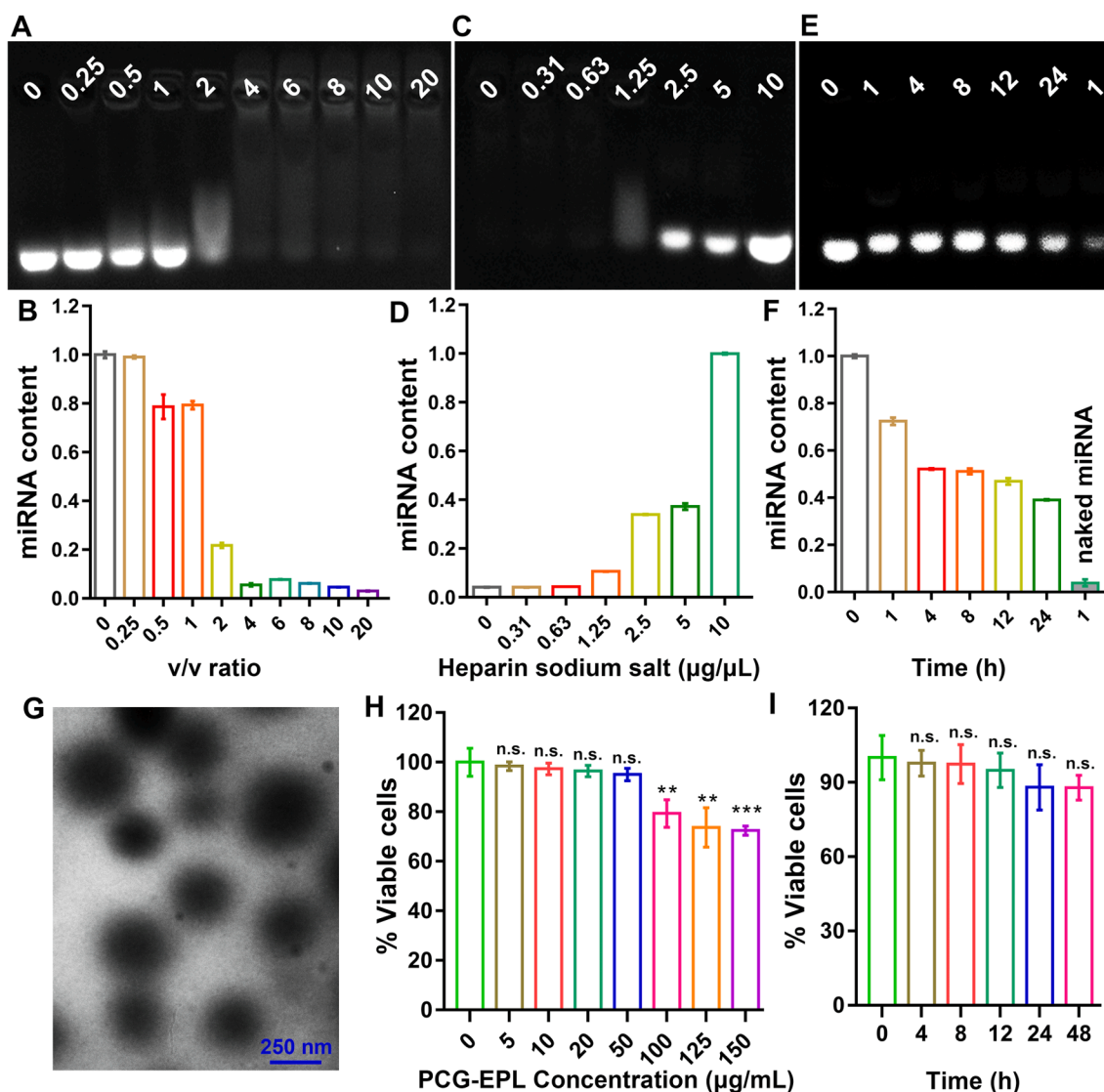


Fig. 2. Preparation and characterizations of PCG-EPL/miR33 nanocomplex. (A-B) Agarose gel electrophoresis results of PCG-EPL/miRNA complexes at various v/v ratios (0, 0.25, 0.5, 1, 2, 4, 6, 8, 10 and 20), indicating the miRNA binding ability. (C-D) Agarose gel electrophoresis results of PCG-EPL/miRNA with different mass heparin sodium salt (0, 0.31, 0.63, 1.25, 2.5, 5 and 10 µg/µL), indicating the miRNA release. (E-F) Agarose gel electrophoresis results of PCG-EPL/miRNA with FBS at different time intervals (0, 1, 4, 8, 12, 24 h and naked miRNA at 1 h), indicating the protecting ability against degradation of enzyme. (G) TEM picture showing the morphology and size of PCG-EPL/miR33 nanocomplex (v/v = 4). (H) Cytotoxicity of PCG-EPL on 3 T3-L1 cells at different concentrations (All data was compared with PEG-EPL at 0 µg/mL concentration). (I) Cytotoxicity of PCG-EPL (50 µg/mL) on 3 T3-L1 cells at different time points (All data was compared with cell treatment at 0 h). Data were expressed as mean ± SD. n.s. (no significance). ** $P < 0.01$, *** $P < 0.001$ (n = 3).

PCG-EPL/miR33mimic negative control), the lipid expression in Lipo/miR33mimic and PCG-EPL/miR33mimic group was significantly down-regulated (Fig. 4A-B). The expressions of IL-1 β , leptin and PPAR- γ were detected by the real-time PCR method. Compared with the control groups, the expressions of IL-1 β (Fig. 4C) and leptin (Fig. 4D) significantly decreased while PPAR- γ (Fig. 4E) significantly increased in the groups treated with miR33 mimic. Additionally, the IL-1 β and leptin genes were significantly down-regulated and the PPAR- γ was significantly up-regulated in PCG-EPL/miR33mimic group compared with Lipo2000/miR33 mimic group, which suggests that PCG-EPL may have higher transfection efficiency of miR33mimic than commercial Lipo 2000.

3.4. Tissue toxicity and gene delivery on fat in vivo

Before analysing the *in vivo* anti-obesity capacity, we evaluated the *in vivo* tissue toxicity of PCG-EPL/miR33agomir nanocomplex. Mice were

injected with PCG-EPL/miR33agomir (10 mg/kg) through the tail vein every two days for 10 times. Then spleen and lung tissues of mice were collected for hematoxylin-eosin (H&E) staining (Fig. 5A). And the results showed that there was no significant difference in tissue integrity and cell structure. It means that PCG-EPL/miR33agomir has no toxic effect on main tissues. According to PCG-EPL/miR33 construction method, we used Cy5 fluorescent labelled RNA to construct PCG-EPL/Cy5RNA to evaluate the *in vivo* gene delivery. After intravenous injection of PEG-EPL/Cy5RNA for 6 h and 8 h, the fluorescence images of major organs and abdominal fat were detected. The fluorescence signals could be detected in the abdominal fat (Fig. 5B). The *ex vivo* semi-quantitative analysis of fluorescence biodistribution is shown in Fig. 5C. The result showed that PCG-EPL can deliver RNA drugs to the abdominal fat after intravenous injection.

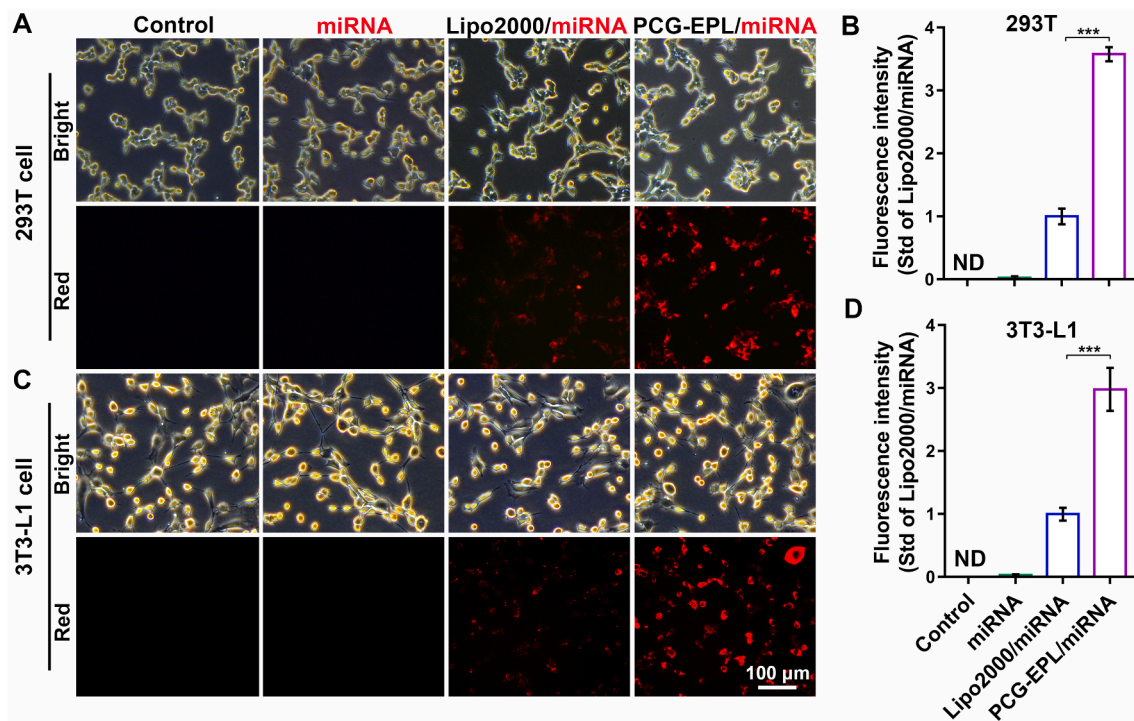


Fig. 3. Cell uptake ability of PCG-EPL/miRNA both in 293T and 3T3-L1 cells. The cy3 fluorescence-labeled negative control miRNA was used to detect the cell uptake ability of PCG-EPL/miRNA both in 293T and 3T3-L1 cells. (A-B) Bright-field and fluorescent images (A) of 293T cells and corresponding relative transfection efficiency results of red fluorescence-labeled cells (miRNA: red). (C-D) Bright-field and fluorescent images (C) of 3T3-L1 cells and corresponding relative transfection efficiency results of red fluorescence-labeled cells (miRNA: red). Compared with commercial transfection reagent Lipo2000, PEG-EPL (20 $\mu\text{g}/\text{mL}$) showed higher transfection efficiency in 293T and 3T3-L1 cells 12 h after transfection. Data were expressed as mean \pm SD. ND (not detected). *** $P < 0.001$ ($n = 3$). (For interpretation of the references to colour in this figure legend, the reader is referred to the web version of this article.)

3.5. Obesity therapy and maintained blood glucose balance in vivo

The anti-obesity performance was characterized through investigating the blood glucose, body and tissues weight in high fat diet obese mice model. The animal experimental time line is shown in Fig. 6A. And the statistical analysis of body weight in each week was recorded in Table S2. Compared with HFD-Ctrl (PCG-EPL/miR33agomir NC), the body weight, abdominal fat (white adipose tissue in the abdominal cavity of the mouse that near the spine side) and liver weight of mice in the HFD-Exp (PCG-EPL/miR33agomir) group were reduced (Fig. 6B-D and 6G-K). But there were no significant differences in the shape and weight between lung and spleen (Fig. 6E-F and 6L-M). Compared with body weight changes on day 1 and day 20, we found that PCG-EPL/miR33agomir significantly reduced body weight (Fig. 6H). Compared with NCD group, the body weight of mice in obese-free mice group (HFD-L, which were fed high-fat diet in the whole process) did not increase significantly (Fig. 6H), which indicated that mice in HFD-L group could effectively control weight gain even if they were fed with high-fat diet. The average body weight of mice in the HFD-Exp group was decreased by 16.42% (Fig. 6I). Through the analysis of the weight of abdominal fat, liver, lung and spleen in mice, the main cause of weight loss was the decrease of abdominal fat (Fig. 6J-M). The total food intake in HFD-Exp group was higher than that in other three groups, but the energy conversion rate was the lowest (Table S3), which suggests that the effect of PCG-EPL/miR33agomir was not to control appetite, but to enhance fat metabolism to achieve weight loss.

To directly test the effect of PCG-EPL/miR33agomir on the glucose tolerance *in vivo*, three mice in each group were randomly selected to fast overnight on day 20. Then mice were given acute injection of glucose followed by an intraperitoneal glucose tolerance test (IPGTT). The blood glucose level was measured at 0, 15, 30, 60, and 120 min after injected with 2 g/kg glucose intraperitoneally. The results showed that

PCG-EPL/miR33agomir could maintain blood glucose balance compared with HFD-Ctrl group (Fig. 6N-O).

3.6. Regulation of fat metabolism in vivo

The changes of morphology and organs weight of mice further arouse our interest to study the anti-obesity effect of PCG-EPL/miR33agomir in histological levels. H&E staining of abdominal fat showed that the adipocytes size in the HFD-Ctrl group was much larger than that in the other three groups (Fig. 7A). According to the statistical results of adipocytes size, PCG-EPL/miR33agomir significantly inhibited adipocytes growth (Fig. 7B-C). After PCG-EPL/miR33agomir therapy, there was no significant difference between HFD-Exp group and HFD-L group.

To further assess the effect of obesity-related proteins in adipocytes, we detected the expression of adiponectin and leptin by double immunofluorescence (Fig. 7D). The adiponectin expression in obese group (HFD-Ctrl) was lower than that in the anti-obesity therapy group (HFD-Exp) (Fig. 7E). Compared with HFD-Ctrl, the expression of leptin in HFD-Exp group was decreased to the same level as that in NCD group (Fig. 7F). To quantify the obesity-related genes expression at the mRNA level, we quantified leptin, IL-1 β , PPAR- γ , fatty acid synthetase (FAS), TNF- α , IL-6 and IL-10 expression in adipocytes (Fig. 7G and Fig. S3A). Compared with HFD-Ctrl group, the IL-1 β , TNF- α and IL-6 expressions in HFD-Exp were decreased, while PPAR- γ and IL-10 expressions significantly increased in adipocytes. The high expressions of leptin and Fas were observed in adipocytes of obese group. These results indicated that PCG-EPL/miR33agomir could significantly reduce the expression of obese related proteins and genes.

3.7. Inflammation regulation in liver and serum

As another important organ, liver plays an important role in lipid

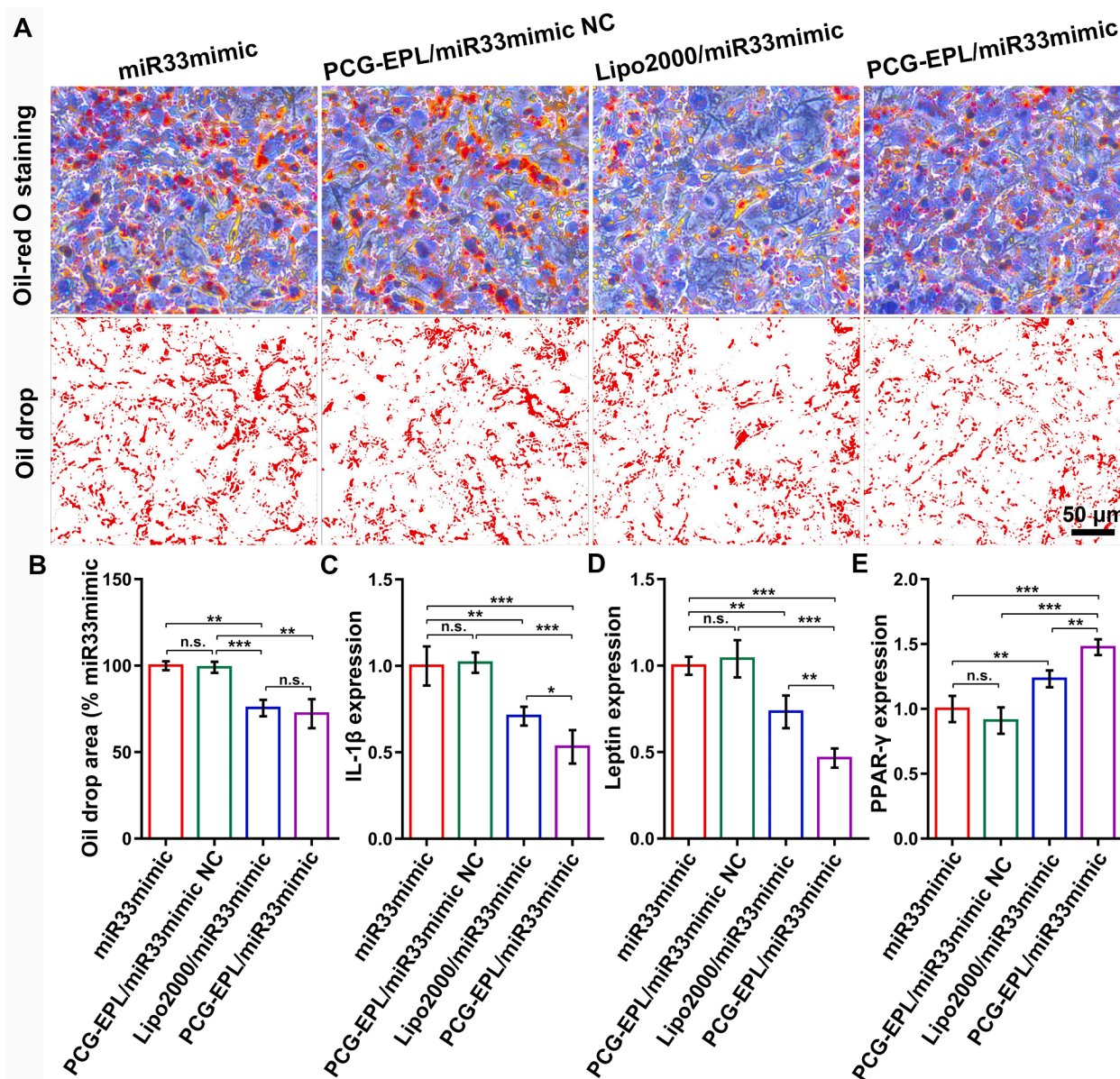


Fig. 4. PCG-EPL/miR33 mimic increased lipid metabolism in adipocytes. The function of PCG-EPL/miR33 mimic on inhibition of lipid expression was evaluated by Oil-Red O Staining and RT-qPCR after incubation with samples (containing 20 nM RNA) for 24 h. (A) Oil-Red O staining indicating the oil drop distribution (red area) in adipocytes. (B) Quantified oil drop area by ImageJ software. (C-E) Expression of IL-1 β (C), leptin (D) and PPAR- γ (E) in adipocytes was measured by RT-qPCR. Data were expressed as mean \pm SD. n.s. (no significance). * $P < 0.05$, ** $P < 0.01$, *** $P < 0.001$ ($n = 3$). (For interpretation of the references to colour in this figure legend, the reader is referred to the web version of this article.)

metabolism. H&E staining showed that there was a large amount of fat around the hepatocytes in the HFD-Ctrl group, which made the gap between hepatocytes larger (Fig. 8A). The results of immunofluorescence showed that the highest expression of IL-1 β and the lowest expression of PPAR- γ were found in the liver tissue of obese group (Fig. 8B-C). After treatment with PCG-EPL/miR33agomir, the expressions of PPAR- γ and IL-10 were increased, while IL-1 β , TNF- α and IL-6 expressions related to inflammation were decreased significantly in liver tissue of HFD-Exp (Fig. 8B-D and Fig. S3B). Those results showed that PCG-EPL/miR33agomir could effectively down regulate the inflammatory response in the liver of obese mice. And our results were consistent with the previous study that obesity was associated with the inflammation and chronically elevated IL-1 β expression [27].

To determine whether systemic obesity-related proteins secretion in serum was affected by PCG-EPL/miR33agomir, ELISA analysis was performed to quantify the serum level of HDL (high-density lipoprotein),

LDL (low-density lipoprotein), leptin and insulin. The expression of these four proteins (HDL, LDL, leptin and insulin) in obese mice serum was higher than those in HFD-Exp, NCD control and obese-free (HFD-L) mice (Fig. 9). These results suggested that PCG-EPL/miR33agomir can systematically down regulate the expression of lipid metabolism related proteins through blood circulation.

4. Discussion

In this study, we developed a biocompatible and biodegradable PCG-EPL polymer for delivering the therapeutic miR33 gene for obesity therapy. The results showed that PCG-EPL polymer could efficiently load/release miR33 and protect it against degradation. PCG-EPL/miR33 nanocomplex was safe and nontoxic both in cellular and tissue level *in vitro* and *in vivo*. PCG-EPL could efficiently deliver miR33 into adipocytes and significantly down-regulate the expression of lipid *in vitro* and

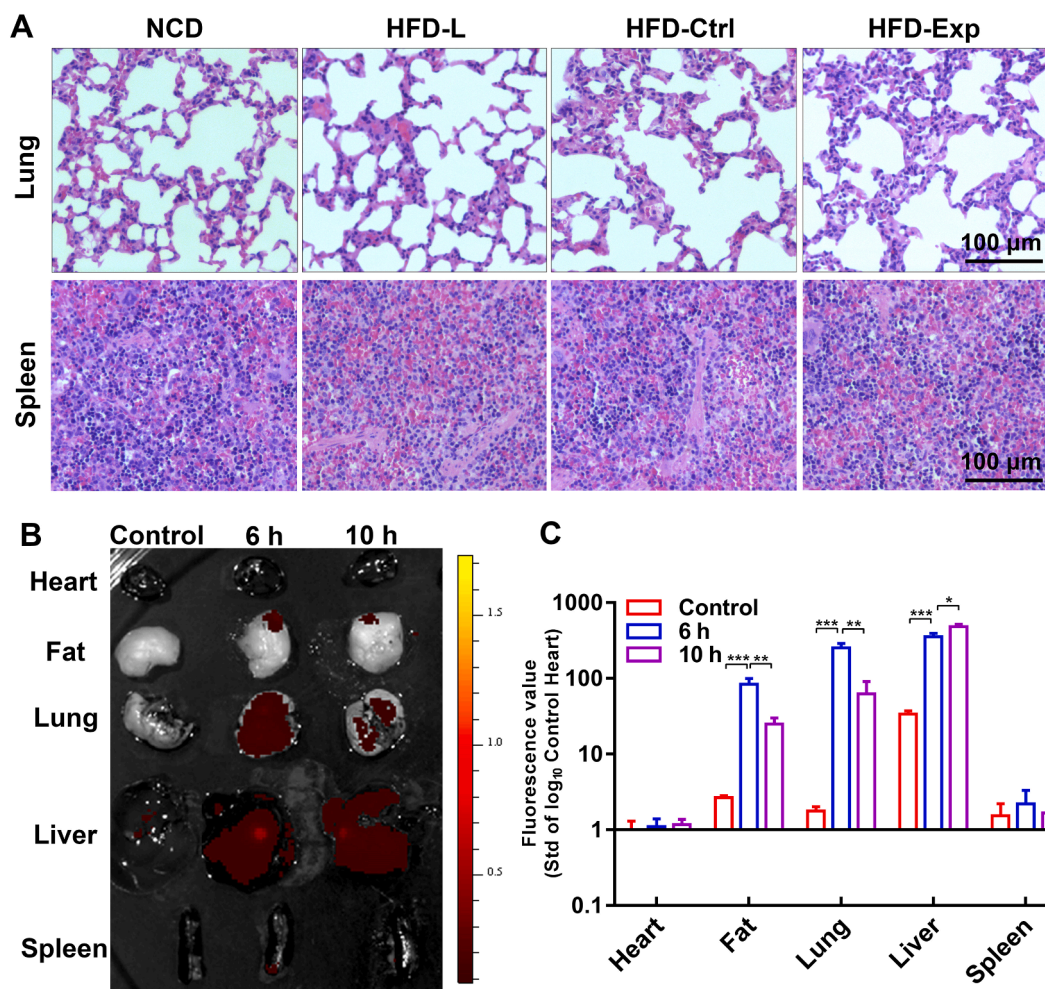


Fig. 5. Tissue toxicity and gene delivery *in vivo* after intravenous injection. (A) Mice were injected with 10 mg/kg PCG-EPL or equal volume PBS through the tail vein every two days for 10 times. Then the lung and spleen of mice were collected for H&E staining. NCD (normal chow diet control) treated with PBS. HFD-L (high fat diet) treated with PCG-EPL/miR33 negative control agomir. HFD-Ctrl (high fat diet) treated with PCG-EPL/miRNC negative control agomir. HFD-Exp (high fat diet) treated with PCG-EPL/miR33 agomir (n = 4). The biodistribution of nanocomplex was detected after intravenous injection of Cy5 labeled PCG-EPL/RNA (2 mg PCG-EPL with 2 nmol Cy5RNA). (B) Representative *ex vivo* fluorescence image of major organs and abdominal fat at 6 h and 10 h after intravenous injection of PEG-EPL/Cy5RNA. (C) *Ex vivo* semi-quantitative analysis of fluorescence biodistribution. Fluorescence value in each organ was determined using Living Image software from PerkinElmer IVIS. Data were expressed as mean \pm SD (n = 3). **P < 0.01, ***P < 0.001.

in vivo. PCG-EPL/miR33 agonist effectively reduced the high fat diet-induced body weight by enhancing lipid metabolism and regulating inflammatory reaction [27].

Diet-induced obesity represents a pre-diabetic state with overweight, lipid accumulation and inflammation [28]. Therefore, body weight, lipid metabolism and inflammation protein can be used as reference factors to evaluate obesity therapy. In this study, the body weight and abdominal fat weight were reduced after 3 weeks of PCG-EPL/miR33 agomir therapy (Fig. 6). Through the analysis of the weight of abdominal fat, liver, lung and spleen in mice, the main cause of weight loss was the decrease of abdominal fat (Fig. 6B-M). The total food intake in HFD-Exp group was higher than that in other three groups, but the energy conversion rate was the lowest (Table S3). This suggests that the effect of PCG-EPL/miR33agomir is not to suppress appetite, but to enhance fat metabolism to achieve weight loss.

As a regulator of inflammatory response, IL-1 β plays important roles in various diseases such as rheumatoid arthritis, inflammatory bowel diseases and type 1 diabetes, atherosclerosis and type 2 diabetes [29]. Obesity is associated with inflammation and circulating IL-1 β concentrations were elevated in obesity mice. Elevated concentrations of glucose and other metabolites drive the production of IL-1 β by macrophages. Blocking IL-1 β with IL-1Ra could improve glycemic control and

β -cell function in diet-induced obesity mice [27]. Peroxisome proliferators-activated receptor- γ (PPAR- γ) is a ligand-inducible transcription factor that exerts glucose and lipid metabolism regulation, anti-inflammatory and anti-oxidant properties [30,31]. Down-regulation of vascular PPAR- γ enhanced inflammation in response to pro-inflammatory cytokines, resulting in endothelial dysfunction. In contrast, over expression of vascular PPAR- γ was protected against inflammatory cytokine IL-1 β -induced endothelial dysfunction through inhibition of oxidative stress [32,33]. And PPAR- γ expression and activity are down-regulated in the peripheral tissues such as colons or adipose tissue in high-fat diet induced obesity mice [34]. In this study, we found that the expression of IL-1 β decreased when inhibiting the lipid expression in adipocytes with PCG-EPL/miR33mimic (Fig. 4C). The *in vivo* results also showed that the expressions of IL-1 β , TNF- α and IL-6 in liver, abdominal adipose in the PCG-EPL/miR33agomir therapy group were significantly lower than that in the obese group (Fig. 7G, 8B-D, and S3). In contrast to IL-1 β , PPAR- γ and IL-10 were up regulated in liver and abdominal adipose after PCG-EPL/miR33agomir treatment (Fig. 7G, 8B-D and S3). These results suggested that the PCG-EPL/miR33 induced downregulation of inflammatory response was probably one of reasons on efficient obesity therapy.

Leptin is associated in body energy homeostasis, and the fed levels of

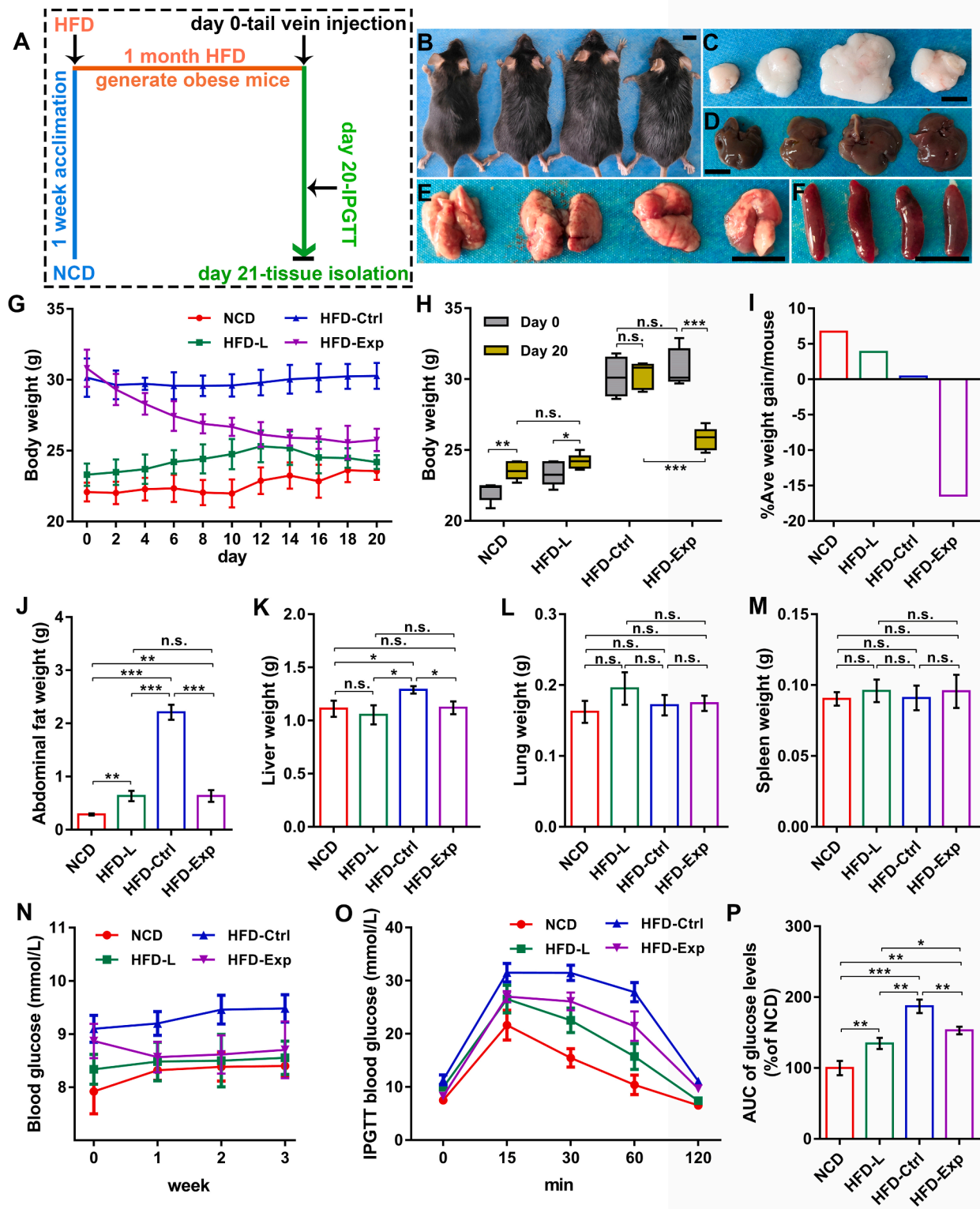


Fig. 6. PCG-EPL/miR33 agomir regulated body weight and circulating blood glucose concentration in HFD-induced obese mice. Mice were injected with 10 mg/kg PCG-EPL or equal volume PBS through the tail vein every two days for 10 times. (A) Timeline of animal experiment. (B-F) Morphological differences of mice (B), abdominal fat (C), liver (D), lung (E) and spleen (F) on day 21 (Group NCD, HFD-L, HFD-Ctrl and HFD-Exp from left to right). All scale bar = 1 cm. (G) Body weight change of mice from day 0 to day 20. (H) Body weight of mice on day 0 and on day 20. (I) Percentage of average weight gains per mouse between day 0 and day 20. (J-M) Tissues weight of abdominal fat (J), liver (K), lung (L) and spleen (M) on day 21. (N) Serial changes in circulating blood glucose levels in 3 weeks (B-N, $n = 7$). (O) IPGTT glucose levels and (P) area under curve (AUC) of glucose levels after intraperitoneal injection of glucose. Glucose tolerance test (GTT) was measured at 0, 15, 30, 60, and 120 min after injected with 2 g/kg glucose intraperitoneally (O-P, $n = 3$). Data were expressed as mean \pm SD. n.s. (no significance). * $P < 0.05$, ** $P < 0.01$, *** $P < 0.001$.

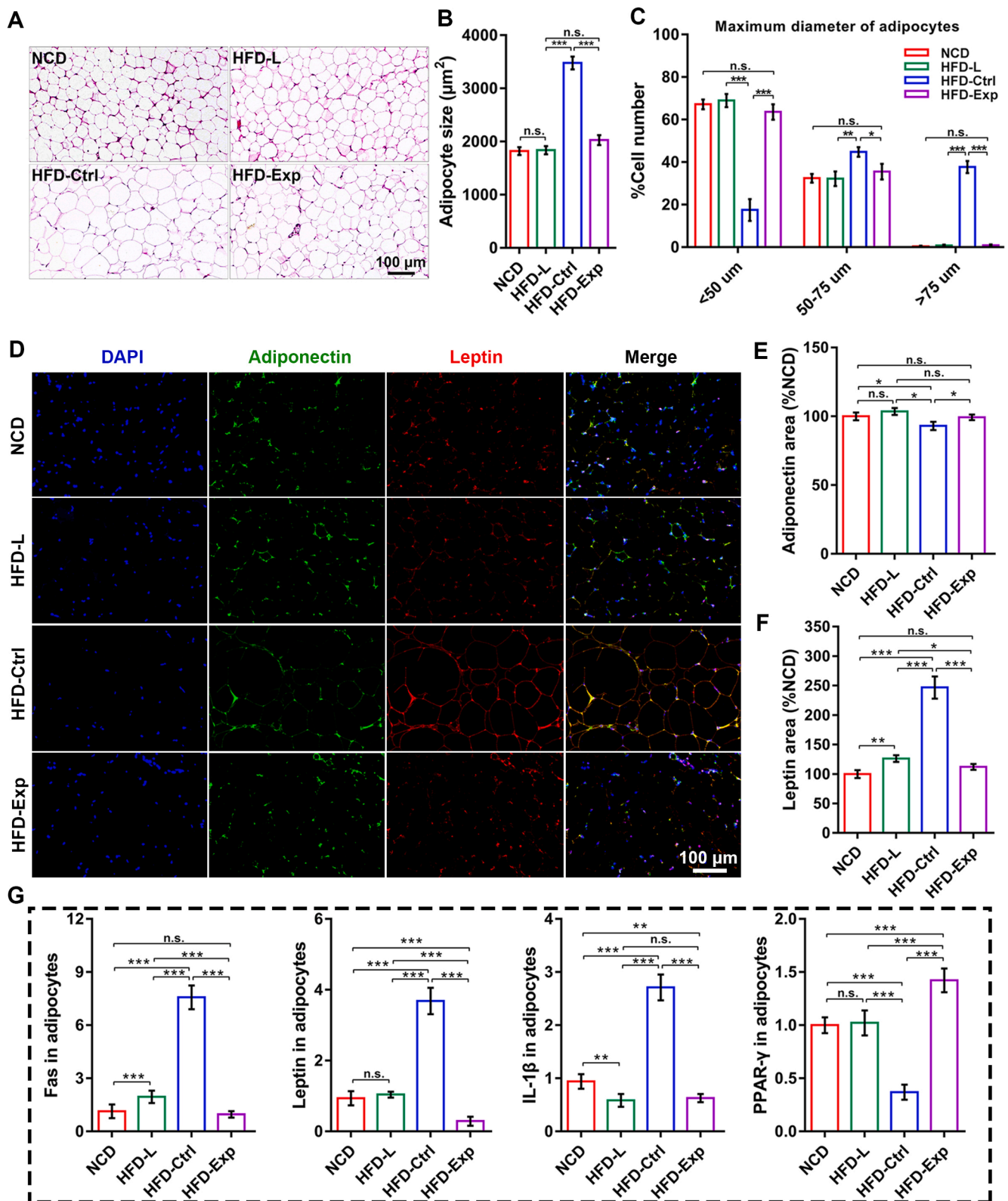


Fig. 7. PCG-EPL/miR33 agomir regulated lipid metabolism in abdominal adipose tissue. On day 21, abdominal adipose tissues were collected for lipid metabolism analysis. (A) H&E staining of abdominal adipose tissue. (B) Mean size and (C) size distribution of adipocytes (μm^2). (D) Double immunofluorescence to detect adiponectin (green) and leptin (red) expression in adipocytes (nuclear: blue by DAPI). (E-F) Quantification of adiponectin (E) and leptin (F) fluorescence intensity. (G) Expressions of leptin, IL-1 β , PPAR- γ and FAS in abdominal adipose. Data were expressed as mean \pm SD. n.s. (no significance). * $P < 0.05$, ** $P < 0.01$, *** $P < 0.001$ ($n = 4$). (For interpretation of the references to colour in this figure legend, the reader is referred to the web version of this article.)

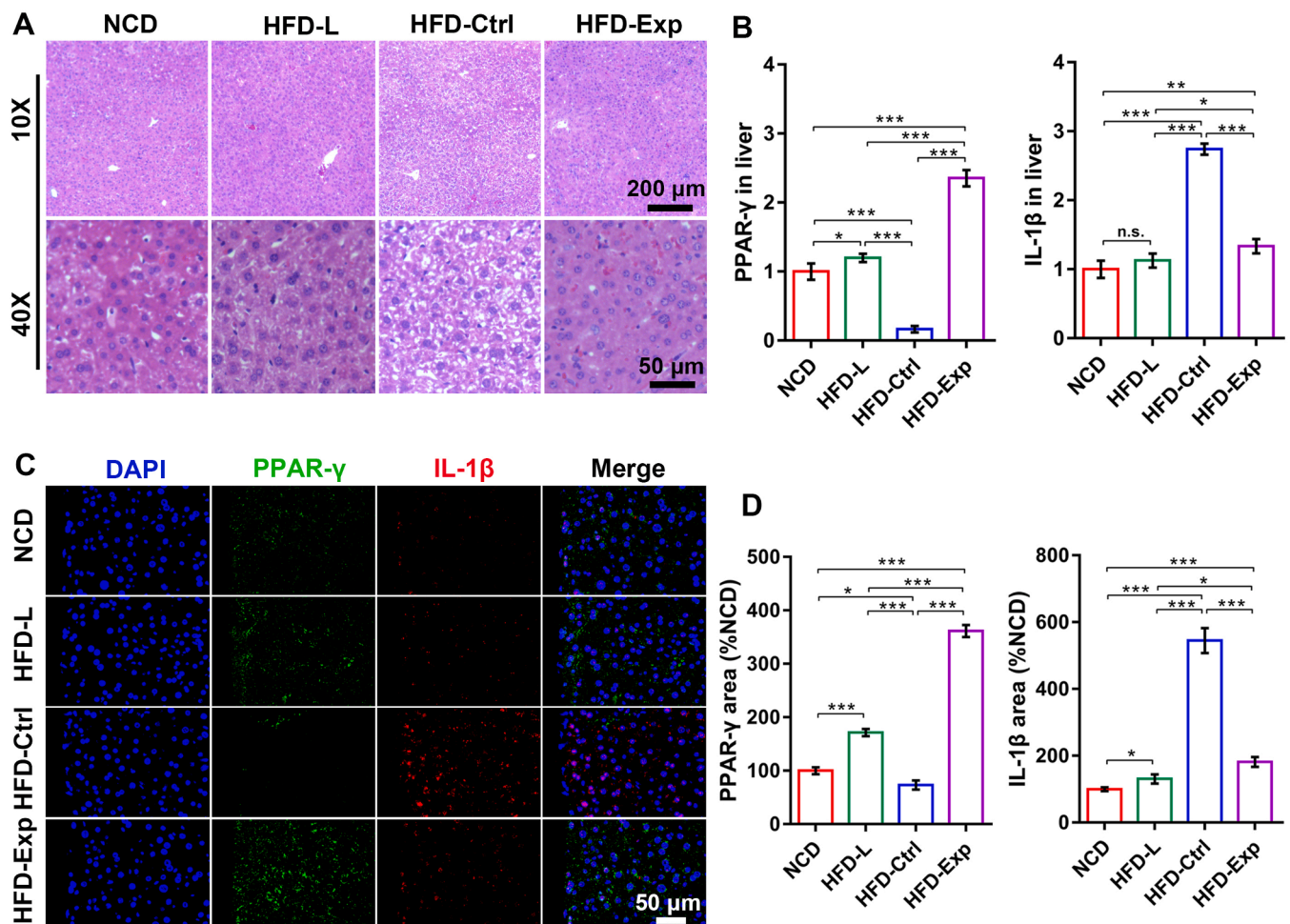


Fig. 8. PCG-EPL/miR33 agomir inhibited the inflammatory response in obese mice liver. On day 21, the liver tissues were collected. (A) H&E staining of liver tissue. (B) Quantified expression of IL-1β and PPAR-γ at the mRNA level in liver tissue. (C) Double immunofluorescence to detect PPAR-γ (green) and IL-1β (red) expression at the protein level in liver tissue (the nuclear was stained as blue by DAPI). (D) Quantification of PPAR-γ and IL-1β fluorescence intensity. Data were expressed as mean ± SD. n.s. (no significance). * $P < 0.05$, ** $P < 0.01$, *** $P < 0.001$ ($n = 4$). (For interpretation of the references to colour in this figure legend, the reader is referred to the web version of this article.)

leptin were significantly increased in miR33 deficient mice [8]. Although leptin could enhance the reduction in food intake, the high consistently levels also could promote the leptin resistance. Leptin is secreted from adipose tissue and these changes are likely due to the increased mass of adipose tissue in these animals [35,36]. However, contrarily to other adipokines, adiponectin was decreased in obesity and correlated directly with insulin sensitivity [37]. We found that after treatment with PCG-EPL/miR33 agomir, adiponectin in adipose tissue was slightly higher than that in obese mice (Fig. 7), while the expression of leptin was significantly inhibited. In addition, circulating high-density lipoprotein (HDL), low-density lipoprotein (LDL) and insulin in obesity therapy mice were down regulated compared with obese mice (Fig. 9). Although inhibition of miR33 could increase circulating HDL and reduce atherosclerotic plaque burden [38], the increase of HDL was accompanied by the increase of LDL expression [39]. Compared with the miR33 deficient mice, the expressions of LDL and HDL were decreased in miR33 over-expressed mice [39], which was consistent with our results that LDL and HDL was decreased in HFD-Exp compared with HFD-Ctrl.

In preparation of obese model mice, we found that some mice were not obese even though they were fed with high-fat diet. In order to study the obese-free mice, we listed them in a single group (HFD-L, which was fed high-fat diet in the whole process). As far as we know, this is the first time to study obese-free mice in anti-obesity therapy studies. Compared with obese mice, although the average energy conversion rate of obese-

free mice was higher, the body weight and food intake were significantly lower (Table S3). And these individuals also performed very well in maintaining blood glucose stability and glucose tolerance (Fig. 6N-O). From the perspective of energy conversion, an important way to lose weight is to control diet. From gene and protein levels, these mice can better maintain the dynamic balance of pro-inflammatory and anti-inflammatory reactions than fat prone mice. Low expression of pro-inflammatory IL-1β and high expression of anti-inflammatory gene PPAR-γ may control the inflammatory response induced by high-fat diet [27]. Compared with normal chow diet group, even if fed with high-fat diet, the ability of obese-free mice to maintain lipid metabolism balance not only benefits from the high expression of HDL, but also from the relatively low level of LDL (Fig. 9).

There were also some limitations in this work as shown below. Firstly, although we have found that PCG-EPL/miR33 can reduce weight without controlling appetite, it is unknown whether this method has any effect on the hypothalamus and another neurosexual organ and adipose tissue transformation related to weight loss. Secondly, the safety and the long-term weight control of this gene therapy need to be verified by more comprehensive testing. Although lots of miRNA mimics have been used in many preclinical studies [40–43], it is worth further studying by increasing the tissue specificity of the drug delivery system.

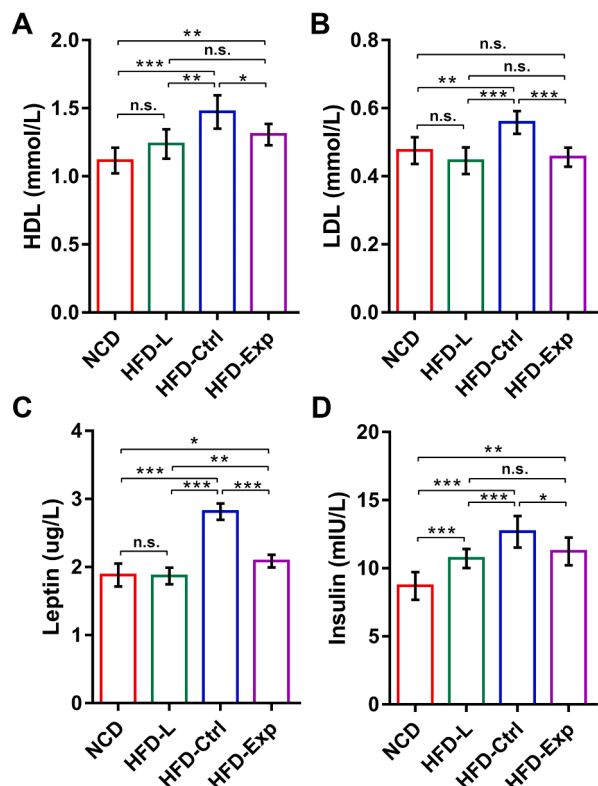


Fig. 9. Obesity related proteins expression in mice serum after injection of PCG-EPL/miR33 agomir for 10 times. (A) HDL, (B) LDL, (C) Leptin, (D) Insulin. Data were expressed as mean \pm SD. n.s. (no significance). * $P < 0.05$, ** $P < 0.01$, *** $P < 0.001$ ($n = 7$).

5. Conclusions

In conclusion, we developed a biocompatible and biodegradable PCG-EPL polymer for delivering the therapeutic miR33 gene for obesity therapy. The results showed that PCG-EPL polymer could efficiently load/release miR33 and protect it against degradation. PCG-EPL/miR33 nanocomplex was safe and nontoxic both in cellular and tissue level *in vitro* and *in vivo*. PCG-EPL could efficiently deliver miR33 into adipocytes and significantly down-regulate the expression of lipid *in vitro* and *in vivo*. PCG-EPL/miR33 agonist can effectively reduce the high fat diet-induced body weight by enhancing lipid metabolism and regulating inflammatory reaction. This study brings good news to obese patients, especially for those who are required to lose weight but are unable to autonomously control their diet.

Declaration of Competing Interest

The authors declare that they have no known competing financial interests or personal relationships that could have appeared to influence the work reported in this paper.

Acknowledgements

This work was supported by National Natural Science Foundation of China (Grant No. 51872224), Key Laboratory of Shaanxi Province for Craniofacial Precision Medicine Research, College of Stomatology, Xi'an Jiaotong University (Grant No. 2018LHM-KFKT004), Special Guidance Funds for the Construction of World-class Universities (disciplines) and Characteristic Development in Central Universities (grant No. PY3A078). The Fundamental Research Funds for the Central Universities (Grant No. xzy022019050). Wenzhou Science and Technology Bureau Project (Grant No. ZY2019003, Y20190123, Y2020236).

Author contributions

L.Z., M.W., and M.C. performed the experiments *in vivo*. L.Z., W.N., T. T.L. and W.G.L performed *in vitro* experiments. L.Z. and M.W. performed the synthesis and assembly of nanomaterials. All authors discussed the data. L.Z. and B.L. prepared figures and wrote the manuscript. L.Z. and B.L. designed and drafted the work.

Appendix A. Supplementary data

Supplementary data to this article can be found online at <https://doi.org/10.1016/j.cej.2020.127304>.

References

- [1] R.S. Padwal, S.R. Majumdar, Drug treatments for obesity: orlistat, sibutramine, and rimonabant, *Lancet* 369 (2007) 71–77, [https://doi.org/10.1016/S0140-6736\(07\)60033-6](https://doi.org/10.1016/S0140-6736(07)60033-6).
- [2] G.A. Bray, K.K. Kim, J.P.H. Wilding, Obesity: A chronic relapsing progressive disease process. A position statement of the world obesity federation, *Obes. Rev.* 18 (2017) 715–723, <https://doi.org/10.1111/obr.12551>.
- [3] J.L. Sonnenburg, F. Bäckhed, Diet–microbiota interactions as moderators of human metabolism, *Nature* 535 (2016) 56–64, <https://doi.org/10.1038/nature18846>.
- [4] A. Elagizi, S. Kachur, C.J. Lavie, S. Carbone, A. Pandey, F.B. Ortega, R.V. Milani, An overview and update on obesity and the obesity paradox in cardiovascular diseases, *Prog. Cardiovasc. Dis.* 61 (2018) 142–150, <https://doi.org/10.1016/j.pcad.2018.07.003>.
- [5] K.B. Kaufmann, H. Büning, A. Galy, A. Schambach, M. Grez, Gene therapy on the move, *EMBO Mol. Med.* 5 (2013) 1642–1661, <https://doi.org/10.1002/emmm.201202287>.
- [6] A.M. Näär, MiR-33: A metabolic conundrum, *Trends Endocrinol. Metab.* 29 (2018) 667–668, <https://doi.org/10.1016/j.tem.2018.04.004>.
- [7] T. Horie, T. Nishino, O. Baba, Y. Kuwabara, T. Nakao, M. Nishiga, S. Usami, M. Izuhara, N. Sowa, N. Yahagi, H. Shimano, S. Matsumura, K. Inoue, H. Marusawa, T. Nakamura, K. Hasegawa, N. Kume, M. Yokode, T. Kita, T. Kimura, K. Ono, MicroRNA-33 regulates sterol regulatory element-binding protein 1 expression in mice, *Nat. Commun.* 4 (2013) 2883, <https://doi.org/10.1038/ncomms3883>.
- [8] N.L. Price, A.K. Singh, N. Rotllan, L. Goedeke, A. Wing, A. Canfrán-Duque, A. Diaz-Ruiz, E. Araldi, á. Baldán, J.P. Camporez, Genetic ablation of miR-33 increases food intake, enhances adipose tissue expansion, and promotes obesity and insulin resistance, *Cell Rep.* 22 (2018) 2133–2145, doi: 10.1016/j.celrep.2018.01.074.
- [9] D. Karunakaran, L. Richards, M. Geoffrion, D. Barrette, R.J. Gotfrid, M.-E. Harper, K.J. Rayner, Therapeutic inhibition of miR-33 promotes fatty acid oxidation but does not ameliorate metabolic dysfunction in diet-induced obesity, *Arterioscl. Throm. Vas.* 35 (2015) 2536–2543, <https://doi.org/10.1161/ATVBAHA.115.306404>.
- [10] K.J. Rayner, C.C. Esau, F.N. Hussain, A.L. McDaniel, S.M. Marshall, J.M. van Gils, T.D. Ray, F.J. Sheedy, L. Goedeke, X. Liu, O.G. Khatsenko, V. Kaimal, C.J. Lees, C. Fernandez-Hernando, E.A. Fisher, R.E. Temel, K.J. Moore, Inhibition of miR-33a/b in non-human primates raises plasma HDL and lowers VLDL triglycerides, *Nature* 478 (2011) 404–407, <https://doi.org/10.1038/nature10486>.
- [11] K.A. High, M.G. Roncarolo, Gene therapy, *New Engl. J. Med.* 381 (2019) 455–464, <https://doi.org/10.1056/NEJMr1706910>.
- [12] Y. Guo, L. Zhou, M. Wang, Y. Li, B. Lei, Biodegradable antibacterial branched glycerol-polypeptide with efficient *in vitro/in vivo* miRNA-29b delivery for promoting osteogenic differentiation of stem cells and bone regeneration, *Chem. Eng. J.* 405 (2021) 127085, <https://doi.org/10.1016/j.cej.2020.127085>.
- [13] P.P.G. Guimarães, S. Gaglione, T. Sewastianik, R.D. Carrasco, R. Langer, M. J. Mitchell, Nanoparticles for immune cytokine TRAIL-based cancer therapy, *ACS Nano* 12 (2018) 912–931, <https://doi.org/10.1021/acs.nano.7b05876>.
- [14] M. Wang, Y. Guo, Y. Xue, W. Niu, M. Chen, P. Ma, B. Lei, Engineering multifunctional bioactive citric acid-based nanovectors for intrinsic targeted tumor imaging and specific siRNA gene delivery *in vitro/in vivo*, *Biomaterials* 199 (2019) 10–21, <https://doi.org/10.1016/j.biomaterials.2019.01.045>.
- [15] Y.L. Chen, S. Zhu, L. Zhang, P.J. Feng, X.K. Yao, C.G. Qian, C. Zhang, X.Q. Jiang, Q. D. Shen, Smart conjugated polymer nanocarrier for healthy weight loss by negative feedback regulation of lipase activity, *Nanoscale* 8 (2016) 3368–3375, <https://doi.org/10.1039/C5NR06721A>.
- [16] C.W. Ng, J. Li, K. Pu, Recent progresses in phototherapy-synergized cancer immunotherapy, *Adv. Funct. Mater.* 28 (2018) 1804688, <https://doi.org/10.1002/adfm.201804688>.
- [17] X. Zhen, C. Xie, Y. Jiang, X. Ai, B. Xing, K. Pu, Semiconducting photothermal nanoagent for remote-controlled specific cancer therapy, *Nano Lett* 18 (2018) 1498–1505, <https://doi.org/10.1021/acs.nanolett.7b05292>.
- [18] J. Yang, Q. Zhang, H. Chang, Y. Cheng, Surface-engineered dendrimers in gene delivery, *Chem. Rev.* 115 (2015) 5274–5300, <https://doi.org/10.1021/cr500554t>.
- [19] W. Huang, X. Wang, C. Wang, L. Du, J. Zhang, L. Deng, H. Cao, A. Dong, Structural exploration of hydrophobic core in polycationic micelles for improving siRNA delivery efficiency and cell viability, *J. Mater. Chem. B* 7 (2019) 965–973, <https://doi.org/10.1039/C8TB02706D>.

- [20] S. Liu, Y. Gao, D. Zhou, M. Zeng, F. Alshehri, B. Newland, J. Lyu, J. O'Keefe-Ahern, U. Greiser, T. Guo, F. Zhang, W. Wang, Highly branched poly(β -amino ester) delivery of minicircle DNA for transfection of neurodegenerative disease related cells, *Nat. Commun.* 10 (2019) 3307, <https://doi.org/10.1038/s41467-019-11190-0>.
- [21] Y. Xi, J. Ge, M. Wang, M. Chen, W. Niu, W. Cheng, Y. Xue, C. Lin, B. Lei, Bioactive anti-inflammatory, antibacterial, antioxidative silicon-based nanofibrous dressing enables cutaneous tumor photothermo-chemo therapy and infection-induced wound healing, *ACS Nano* 14 (2020) 2904–2916, <https://doi.org/10.1021/acsnano.9b07173>.
- [22] M. Wang, M. Chen, W. Niu, D.D. Winston, W. Cheng, B. Lei, Injectable biodegradation-visual self-healing citrate hydrogel with high tissue penetration for microenvironment-responsive degradation and local tumor therapy, *Biomaterials* 261 (2020), 120301 doi: 10.1016/j.biomaterials.2017.12.005, doi: 10.1016/j.biomaterials.2020.120301.
- [23] M. Yu, Y. Du, Y. Han, B. Lei, Biomimetic elastomeric bioactive siloxane-based hybrid nanofibrous scaffolds with miRNA activation: a joint physico-chemical-biological strategy for promoting bone regeneration, *Adv. Funct. Mater.* 30 (2020) 1906013, <https://doi.org/10.1002/adfm.201906013>.
- [24] Y. Cao, H.Y. Huang, L.Q. Chen, H.H. Du, J.H. Cui, L.W. Zhang, B.J. Lee, Q.R. Cao, Enhanced lysosomal escape of pH-responsive polyethylenimine–betaine functionalized carbon nanotube for the codelivery of survivin small interfering RNA and doxorubicin, *ACS Appl. Mater. Inter.* 11 (2019) 9763–9776, <https://doi.org/10.1021/acscami.8b20810>.
- [25] C. Jiang, J. Chen, Z. Li, Z. Wang, W. Zhang, J. Liu, Recent advances in the development of polyethylenimine-based gene vectors for safe and efficient gene delivery, *Expert Opin. Drug Del.* 16 (2019) 363–376, <https://doi.org/10.1080/17425247.2019.1604681>.
- [26] K. Kim, K. Ryu, Y.S. Choi, Y.-Y. Cho, J.Y. Lee, H.S. Lee, H. Chang Kang, Effects of the physicochemical, colloidal, and biological characteristics of different polymer structures between α -Poly(L-lysine) and ϵ -Poly(L-lysine) on polymeric gene delivery, *Biomacromolecules* 19 (2018) 2483–2495, <https://doi.org/10.1021/acs.biomac.8b00097>.
- [27] E. Dror, E. Dalmas, D.T. Meier, S. Wueest, J. Thévenet, C. Thienel, K. Timper, T. M. Nordmann, S. Traub, F. Schulze, F. Item, D. Vallois, F. Pattou, J. Kerr-Conte, V. Lavallard, T. Berney, B. Thorens, D. Konrad, M. Böni-Schnetzler, M.Y. Donath, Postprandial macrophage-derived IL-1 β stimulates insulin, and both synergistically promote glucose disposal and inflammation, *Nat. Immunol.* 18 (2017) 283, <https://doi.org/10.1038/ni.3659>.
- [28] J. Zhao, D. Luo, Z. Zhang, N. Fan, Y. Wang, H. Nie, J. Rong, Celastrol-loaded PEG-PCL nanomicelles ameliorate inflammation, lipid accumulation, insulin resistance and gastrointestinal injury in diet-induced obese mice, *J. Control. Release* 310 (2019) 188–197, <https://doi.org/10.1016/j.jconrel.2019.08.026>.
- [29] K. Maedler, G. Dharmadhikari, D.M. Schumann, J. Störting, Interleukin-1 beta targeted therapy for type 2 diabetes, *Expert Opin. Biol. Th.* 9 (2009) 1177–1188, <https://doi.org/10.1517/14712590903136688>.
- [30] R. Marion-Letellier, G. Savoye, S. Ghosh, Fatty acids, eicosanoids and PPAR gamma, *Eur. J. Pharmacol.* 785 (2016) 44–49, <https://doi.org/10.1016/j.ejphar.2015.11.004>.
- [31] W. Wahli, L. Michalik, PPARs at the crossroads of lipid signaling and inflammation, *Trends Endocrin. Met.* 23 (2012) 351–363, <https://doi.org/10.1016/j.tem.2012.05.001>.
- [32] C. Hu, K.T. Lu, M. Mukohda, D.R. Davis, F.M. Faraci, C.D. Sigmund, Interference with PPAR γ in endothelium accelerates angiotensin II-induced endothelial dysfunction, *Physiol. Genomics* 48 (2015) 124–134, <https://doi.org/10.1152/physiolgenomics.00087.2015>.
- [33] M. Mukohda, M. Stump, P. Ketsawatsonkron, C. Hu, F.W. Quelle, C.D. Sigmund, Endothelial PPAR- γ provides vascular protection from IL-1 β -induced oxidative stress, *Am. J. Physiol-Heart C* 310 (2015) H39–H48, <https://doi.org/10.1152/ajpheart.00490.2015>.
- [34] W.X. Liu, T. Wang, F. Zhou, Y. Wang, J.-W. Xing, S. Zhang, S.Z. Gu, L.X. Sang, C. Dai, H.L. Wang, Voluntary exercise prevents colonic inflammation in high-fat diet-induced obese mice by up-regulating PPAR- γ activity, *Biochem. Bioph. Res. Co.* 459 (2015) 475–480, <https://doi.org/10.1016/j.bbrc.2015.02.047>.
- [35] A.C. Köhner, Jens C. Brüning, Selective insulin and leptin resistance in metabolic disorders, *Cell Metab.* 16 (2012) 144–152, <https://doi.org/10.1016/j.cmet.2012.07.004>.
- [36] M.G. Myers, R.L. Leibel, R.J. Seeley, M.W. Schwartz, Obesity and leptin resistance: distinguishing cause from effect, *Trends Endocrin. Met.* 21 (2010) 643–651, <https://doi.org/10.1016/j.tem.2010.08.002>.
- [37] T. Yamauchi, T. Kadowaki, Adiponectin receptor as a key player in healthy longevity and obesity-related diseases, *Cell Metab.* 17 (2013) 185–196, <https://doi.org/10.1016/j.cmet.2013.01.001>.
- [38] L. Goedeke, A. Salerno, C.M. Ramírez, L. Guo, R.M. Allen, X. Yin, S.R. Langley, C. Esau, A. Wanschel, E.A. Fisher, Y. Suárez, A. Baldán, M. Mayr, C. Fernández-Hernando, Long-term therapeutic silencing of miR-33 increases circulating triglyceride levels and hepatic lipid accumulation in mice, *EMBO Mol. Med.* 6 (2014) 1133–1141, <https://doi.org/10.15252/emmm.201404046>.
- [39] N.L. Price, N. Rotllan, A. Canfrán-Duque, X. Zhang, P. Pati, N. Arias, J. Moen, M. Mayr, D.A. Ford, Á. Baldán, Genetic dissection of the impact of miR-33a and miR-33b during the progression of atherosclerosis, *Cell Rep.* 21 (2017) 1317–1330, <https://doi.org/10.1016/j.celrep.2017.10.023>.
- [40] R. Rupaimoole, F.J. Slack, MicroRNA therapeutics: towards a new era for the management of cancer and other diseases, *Nat. Rev. Drug Discov.* 16 (2017) 203–222, <https://doi.org/10.1038/nrd.2016.246>.
- [41] G. Liu, D. Yang, R. Rupaimoole, C.V. Pecot, Y. Sun, L.S. Mangala, X. Li, P. Ji, D. Cogdell, L. Hu, Y. Wang, C. Rodriguez-Aguayo, G. Lopez-Berestein, I. Shmulevich, L. De Cecco, K. Chen, D. Mezzanzanica, F. Xue, A.K. Sood, W. Zhang, Augmentation of response to chemotherapy by microRNA-506 through regulation of rad51 in serous ovarian cancers, *J. Natl. Cancer. Inst.* 107 (2015) 108–130, <https://doi.org/10.1093/jnci/djv108>.
- [42] J.F. Wiggins, L. Ruffino, K. Kelnar, M. Omotola, L. Patrawala, D. Brown, A. G. Bader, Development of a lung cancer therapeutic based on the tumor suppressor microRNA-34, *Cancer Res.* 70 (2010) 5923–5930, <https://doi.org/10.1158/0008-5472.CAN-10-0655>.
- [43] H.P. Joshi, I.V. Subramanian, E.K. Schnetzler, G. Ghosh, R. Rupaimoole, C. Evans, M. Saluja, Y. Jing, I. Cristina, S. Roy, Y. Zeng, V.H. Shah, A.K. Sood, S. Ramakrishnan, Dynamin 2 along with microRNA-199a reciprocally regulate hypoxia-inducible factors and ovarian cancer metastasis, *P. Natl. Acad. Sci. U.S.A.* 111 (2014) 5331–5336, <https://doi.org/10.1073/pnas.1317242111>.